Histone monoaminylation dynamics are regulated by a single enzyme and promote neural rhythmicity

Short title: H3Q5his contributes to brain rhythmicity

One sentence summary: A single enzyme, TGM2, bidirectionally controls H3 monoaminylation dynamics, which, in turn, facilitate neural rhythmicity.

Qingfei Zheng[1!#], Ryan M. Bastle[2#], Shuai Zhao[3#], Lingchun Kong[2], Lauren Vostal[1,4], Aarthi Ramakrishnan[2], Li Shen[2], Sasha L. Fulton[2], Haifeng Wang[3], Baichao Zhang[3], Robert E. Thompson[5], Henrik Molina[6], Stephanie Stransky[7], Simone Sidoli[7], Tom W. Muir[5], Haitao Li[3*], Yael David[1, 4, 8-9*], Ian Maze[2, 10-11*]

[1]**Chemical Biology Program, Memorial Sloan Kettering Cancer Center, New York, New York 10065, USA**
Qingfei Zheng, Lauren Vostal & Yael David

[2]**Nash Family Department of Neuroscience, Friedman Brain Institute, Icahn School of Medicine at Mount Sinai, New York, New York 10029, USA**
Ryan M. Bastle, Lingchun Kong, Aarthi Ramakrishnan, Li Shen, Sasha L. Fulton & Ian Maze

[3]**Beijing Advanced Innovation Center for Structural Biology, MOE Key Laboratory of Protein Sciences, Department of Basic Medical Sciences, School of Medicine, Tsinghua University, Beijing 100084, China**
Shuai Zhao, Haifeng Wang, Baichao Zhang & Haitao Li

[4]**Tri-Institutional PhD Program in Chemical Biology, New York, New York 10065, USA**
Lauren Vostal & Yael David

[5]**Department of Chemistry, Princeton, New Jersey 08544, USA**
Robert E. Thompson & Tom W. Muir

[6]**The Rockefeller University Proteomics Resource Center, The Rockefeller University, New York, NY 10065, USA**
Henrik Molina

[7]**Department of Biochemistry, Albert Einstein College of Medicine, New York, NY 10461, USA**
Stephanie Stransky & Simone Sidoli

[8]**Department of Physiology, Biophysics and Systems Biology, Weill Cornell Medicine, New York, New York 10065, USA**
Yael David

[9]**Department of Pharmacology, Weill Cornell Medicine, New York, New York 10065, USA**
Yael David

[10]Department of Pharmacological Sciences, Icahn School of Medicine at Mount Sinai, New York, New York 10029, USA
Ian Maze

[11]Howard Hughes Medical Institute, Icahn School of Medicine at Mount Sinai, New York, New York 10029, USA
Ian Maze

[!]Current Address: Department of Radiation Oncology, College of Medicine and Center for Cancer Metabolism, James Comprehensive Cancer Center, The Ohio State University, Columbus, Ohio 43210, USA
Qingfei Zheng

[#]Denotes equal contributions

***Corresponding authors**

Ian Maze
Email: ian.maze@mssm.edu

Yael David
Email: davidshy@mskcc.org

Haitao Li
Email: lht@tsinghua.edu.cn

ABSTRACT

Histone H3 monoaminylations at glutamine(Q) 5 represent an important family of epigenetic markers in neurons that play critical roles in the mediation of permissive gene expression. We previously demonstrated that H3Q5 serotonylation(ser) and dopaminylation(dop) are catalyzed by the Transglutaminase 2 (TGM2) enzyme. Here, we found that TGM2 additionally functions as an "eraser" and "re-writer" of H3 monoaminylations, and identified a new class of this modification, H3Q5 histaminylation(his), which displayed dynamic diurnal expression in brain and contributed to neural rhythmicity. We found that H3Q5his, versus H3Q5ser, inhibited binding of the MLL1 complex to the H3 N-terminus and attenuated its methyltransferase activity on H3 lysine(K) 4. We determined that H3Q5 monoaminylation dynamics are dictated by local monoamine concentrations, which are sensed by TGM2. This noncanonical mechanism indicated that histone monoaminylations can be established and removed by a single enzyme based upon its sensing of cellular microenvironments.

MAIN TEXT

Post-translational modifications (PTMs) of histones have emerged as a key regulatory mechanism contributing to diverse DNA-templated processes, including transcription and DNA repair (1). Well-studied PTMs, such as methylation, acetylation and ubiquitination are dynamically regulated by corresponding, site-specific "writer" and "eraser" enzymes and can be recognized by "reader" proteins that facilitate downstream cellular responses (2-3). In addition, various small molecule metabolites can directly react with substrate proteins to form site-specific adducts, or can be indirectly added to amino acid side chains through enzymatic processes (4-6). These modifications can both impact the three-dimensional architecture of chromatin and alter transcriptional landscapes, thereby serving as important mediators of cell fate and plasticity (1-6).

We recently reported on the identification of a new class of histone PTMs, whereby monoamine neurotransmitters, such as serotonin and dopamine (termed serotonylation and dopaminylation, respectively), can be transamidated to glutamine residues (7-12). We specifically determined that histone H3 glutamine (Q) 5 is a primary site of modification and demonstrated that H3 monoaminylations play important roles in regulating neuronal transcriptional programs, both during development and in adult brain (8). We found that H3Q5 serotonylation (H3Q5ser) acts as a permissive mark, both enhancing the recruitment of the general transcription factor complex TFIID to the active mark H3 lysine 4 (K4) tri-methylation (me3), and attenuating demethylation of H3K4 via inhibition of KDM5 family and LSD1 demethylases (8-9). In subsequent studies, we characterized dopaminylation events at this same site (H3Q5dop) in ventral tegmental area (VTA) and found that aberrant accumulation of H3Q5dop during abstinence to drugs of abuse promotes persistent transcriptional programs that facilitate

relapse vulnerability (10-11). Importantly, we uncovered that these monoaminylation events are catalyzed by Transglutaminase 2 (TGM2), a Ca^{2+}-dependent enzyme that exhibits multiple functions, including aminolysis, hydrolysis and alcoholysis of protein glutamine residues, as well as inducing covalent protein crosslinks (13-14). However, the precise enzymatic regulatory mechanisms through which H3 monoaminylation adducts are removed, or exchanged, to allow for neuronal transcriptional plasticity remained poorly understood.

TGM2 is an H3 serotonylation "eraser" in cells

To investigate the regulatory mechanisms of H3 serotonylation dynamics in cells, we utilized the reported 5-propargylated tryptamine (5-PT) chemical probe to track histone serotonylation reactions via Cu(I)-catalyzed azide-alkyne cycloaddition (CuAAC) (8, 15). Initially, we performed a serotonylation pulse-chase experiment to determine the stability of H3ser in cells. We transfected HEK293T cells, which do not endogenously express TGM2, with wild-type (WT) pACEBac1-flag-TGM2 (8). Transfected cells were then treated with 500 μM 5-PT for 6 hours, washed and incubated for an additional 12 hours in 5-PT-free media. Histones were then isolated by high salt extraction, clicked with CuAAC-meditated Cyanine 5 (Cy5), separated by SDS-PAGE and imaged for fluorescence **(Figure 1A)**. Unexpectedly, we observed that the H3ser signal, which was induced in the presence of 5-PT and TGM2-WT, were decreased in TGM2-WT expressing cells during the chase phase, while histones extracted from cells treated with TGM2 inhibitors [ERW1041E (16) or ZDON (17)] did not lose the serotonylation adduct **(Figure 1B)**. These results suggested that in the absence of a serotonin donor, TGM2 may also catalyze the removal of the mark from H3. We confirmed this

observation in HeLa cells, which express TGM2 endogenously, in a similar pulse-chase experiment **(Figure 1C and Supplementary Figure 1)**.

TGM2 is an H3 monoaminylation "re-writer" in vitro

Since our results suggested a serotonylation erasing capability for TGM2, we aimed to test whether this mechanism relies on its canonical catalytic residue, cysteine (Cys) 277, through a nucleophilic attack of the γ-carboxamide group of glutamines **(Figure 2A)**. In this hypothesized mechanism, a thioester intermediate would then activate the amide bond to accept a second nucleophilic attack from donors within the reaction's microenvironment. To test this, we first synthesized H3 N-terminal tail peptides (1-21 amino acids) to act as substrates and product standards for Q5ser, Q5dop and Q5E (the predicted deamidated product) **(Supplementary Figure 2)**. Next, H3Q5ser or H3Q5dop peptides were incubated with lysates from HEK293T cells expressing either TGM2-WT or the catalytically dead mutant, TGM2-C277A. Liquid chromatography-mass spectrometry (LC-MS) analyses revealed that H3Q5ser and H3Q5dop peptides incubated with lysates containing TGM2-WT underwent stoichiometric removal/deamidation [see **Figure 2B, xi** for LC-MS trace of the deamidated product – Q5 to E (glutamic acid) 5] of the serotonylation and dopaminylation adducts. Importantly, the monoaminylated peptides remained unchanged in the presence of lysates from cells expressing the mutant TGM2-C277A enzyme **(Figure 2B, i-iv)**. To provide more insights into the possible biochemical mechanism of TGM2-dependent monoaminylation "re-writing" activity, we purified recombinant TGM2-WT and TGM2-C277A to be used in *in vitro* reactions **(Supplementary Figure 3)**. Next, we incubated either WT or mutant TGM2 enzymes with H3Q5ser or H3Q5dop peptides in the presence of Ca^{2+}. We similarly analyzed these *in vitro* reactions by LC-MS, which

provided consistent results to those observed after cell lysate incubations **(Figure 2B, v-viii)**. Co-immunoprecipitation (Co-IP) experiments performed on recombinant H3 proteins confirmed this unique enzymatic mechanism by capturing the putative TGM2-H3 thioester complex with TGM2-WT but not with TGM2-C277A **(Supplementary Figure 4)**.

Given the "re-writing" activity of TGM2 and the physiological significance of histamine, another monoamine molecule involved in diverse physiological processes ranging from local immune signaling to functions of the gut and neurotransmission (18), we next focused our attention on histamine as a potential alternative donor for histone H3Q5 monoaminylation (H3Q5his). To test whether histamine, like serotonin and dopamine, can act as a cofactor for TGM2 to modify H3Q5, we examined this reaction in a purified system. We incubated WT H3 peptides with recombinant TGM2 (WT or C277A) in the presence of histamine, followed by LC-MS analysis **(Figure 2B, ix-x and Supplementary Figure 5A-D)**. Our results indicated that histamine was stoichiometrically added to the H3 peptide at glutamine 5 (**Supplementary Figure 5**C), consistent with previous reports suggesting that histamine is a preferred donor for TGM2 mediated transamidation of other substrate proteins (19). Moreover, we found that the synthetic H3Q5his peptide was converted to H3Q5E by TGM2-WT in the absence of free histamine **(Figure 2B, xiv and Supplementary Figure 2)** and was fully converted to H3Q5ser **(Figure 2B, xii)** or H3Q5dop **(Figure 2B, xiii)** in the presence of the corresponding monoamine donor. Importantly, we identified the presence of endogenous H3Q5his in HEK293T cells expressing TGM2-WT and treated with histamine**,** but not in cells expressing TGM2-C277A, via LC-MS/MS **(Figure 2C)**.

TGM2 regulates H3Q5his dynamics in vitro and in cells

To identify whether H3Q5his accumulates in cells when histamine is provided as a donor, we generated a polyclonal antibody that selectively recognizes H3Q5his, but not the other monoaminyl marks, *in vitro* and *in vivo* (using cells and brain tissues) – see **Supplementary Figure 6A-E** for antibody validations. We treated HEK293T cells expressing TGM2-WT or TGM2-C277A with histamine, and following cell harvesting, histones were extracted and analyzed by western blot analysis using the new antibody. These results revealed the accumulation of H3Q5his in TGM2-WT expressing cells (*vide infra,* **Figure 3B**).

To further investigate the dynamics of H3Q5his and its regulation by TGM2 in a more physiologically relevant context, we performed an *in vitro* competition assay using reconstituted nucleosome core particles (NCPs) as substrates **(Figure 3A)**. We performed pulse-chase experiments, where we treated NCPs with one monoamine (in this case histamine) and used a buffer exchange column to replace the monoamine donor before the chase. Our results not only indicated that H3Q5his can be efficiently removed from NCPs in a TGM2-dependent manner, but also that the presence of a different monoamine donor during the chase phase resulted in "re-writing" of the mark to alternative monoaminylation states based upon the donor provided. This reaction did not occur in the presence of the TGM2-specific inhibitor, ERW1041E **(Figure 3A)**.

Next, a similar pulse-chase experiment was performed using HEK293T cells expressing TGM2. Histamine was added to the media to allow for H3Q5his establishment, followed by a chase with media containing 5-PT or dopamine. The analysis of H3 monoaminylation, presented in **Figure 3B**, demonstrated that in the

presence of TGM2, H3Q5his was efficiently converted to the alternative monoaminylation state as a function of the donor. Overall, these results indicated that histone monoaminylation is a family of highly dynamic epigenetic modifications that are regulated by a single enzyme, TGM2, based upon the local concentration of monoamine donors within a given cellular context.

H3Q5 histaminylation is enriched in tuberomammillary nucleus and displays dirurnal rhythmicity

To explore the biological significance of H3Q5his dynamics *in vivo*, we turned our investigations to the posterior hypothalamic tuberomammillary nucleus (TMN), which consists largely of histaminergic neurons and is involved in diverse biological functions ranging from control of arousal to maintenance of sleep-wakes cycles and energy balance (20). Indeed, TMN was found to be enriched for H3Q5his *vs.* other non-histaminergic nuclei examined **(Supplementary Figure 6I)**. Given the TMN's prominent role in diurnal behavioral rhythmicity, we first assessed whether the TMN itself displays rhythmic patterns of gene expression that may require chromatin-based control. To do so, we performed bulk tissue RNA-seq on mouse TMN tissues collected at various time points across the zeitgeber (ZT) beginning at time ZT0 hour (the beginning of 'lights on' for mice, which marks the initiation of their inactive phase owing to nocturnalism) and then every 4 hours for 24 hours, with ZT12 marking the beginning of the animals active phase. These RNA-seq data were then analyzed using JTK_CYCLE (21), which is a non-parametric algorithm designed to detect rhythmic components in genome-wide datasets. These analyses revealed that the TMN displays rhythmic gene expression patterns **(Figure 4A)**, with many known circadian genes (e.g., *Arntl*, *Dbp*, *Per1/2*, etc.) identified as being significantly regulated in this manner

(Figure 4B and Supplementary Data 1). Furthermore, ChEA analysis (22), which infers transcription factor regulation from integration of previous genome-wide chromatin immunoprecipitation (ChIP) analyses, identified CLOCK as a robust transcriptional regulator of the genes identified in our rhythmic gene expression dataset **(Figure 4C)**, thereby confirming the histaminergic TMN as a transcriptionally rhythmic brain region.

We next performed western blotting for H3Q5his in TMN across the ZT to determine the mark's expression pattern. We found that H3Q5his is a rhythmic histone modification, with its expression highest during transitions into the active phase and lowest during transitions into the inactive phase for mice **(Figure 4D)**. Such patterns of expression appeared to mimic those of the *Hdc* gene **(Supplementary Figure 7A)** that encodes for the protein Histidine decarboxylase, which mediates the catalysis of histidine to form histamine, suggesting that fluctuations in histamine metabolism may contribute to overall levels of the mark in this brain region.

Given that our previous data indicated that other H3 monoaminylation states often function combinatorially with adjacent H3K4 methylation (specifically H3K4me3) to control transcriptional processes (8-9), we next generated a site-specific antibody that selectively recognizes H3K4me3Q5his (see **Supplementary Figure 6F-H** for antibody validations), followed by expression profiling across the ZT in TMN. We found that H3K4me3Q5his, while present in TMN, does not display a rhythmic pattern of expression, with similar results observed using an H3K4me3 specific antibody, which recognizes H3K4me3 both in the absence and presence of Q5his **(Supplementary Figure 7B)**. H3K4me1 and TGM2 were also found to be non-rhythmic

(Supplementary Figure 7B), providing further evidence that H3Q5his dynamics are a function of histamine availability rather than TGM2 expression. While our data indicated that H3K4me1, H3K4me3 and H3K4me3Q5his were not rhythmic in TMN, previous literature had demonstrated that other valence states of H3K4 methylation, such as H3K4me2, may also contribute to diurnal gene expression (23). As such, we examined H3K4me2 expression across the ZT, and found that not only is H3K4me2 rhythmic but also that its pattern of expression significantly diverges from that of H3Q5his, suggesting that H3Q5his may play an antagonistic role in the regulation of H3K4me2 dynamics **(Figure 4D)**. Finally, to assess whether other brain regions that receive histaminergic projections also display H3Q5his dynamics related to diurnal cycling, we evaluated H3Q5his expression across the ZT in the hypothalamic suprachiasmatic nucleus (SCN), which is considered to be a brain region important for producing circadian rhythms (24). Unlike in TMN, H3Q5his was not found to be rhythmic in SCN **(Supplementary Figure 7C)**.

Diurnal fluctuations of H3Q5his in TMN contribute to molecular and behavioral rhythmicity

We next sought to investigate whether perturbing diurnal rhythms may result in altered regulation of H3Q5his dynamics in TMN, and reciprocally, whether altering H3Q5his may disrupt diurnal gene expression and behavior. To do so, we treated mice pharmacologically with the sleep aid Zolpidem (aka Ambien) at 10 mg/kg during the beginning of the mouse active phase – a perturbation that robustly results in an immediate loss of activity, as measured by locomotor behavior **(Figure 4E).** We then collected TMN tissues 8 hours after treatment for assessments of H3Q5his expression. In vehicle treated controls, comparing H3Q5his expression at ZT8 *vs.* ZT20, we found

that H3Q5his expression is reduced, as expected. However, treatment with Zolpidem significantly attenuated this reduction in expression **(Figure 4F)**, suggesting that the mark's levels are linked to sleep-wake cycles. While H3Q5his expression can be altered by inducing sleep, it remained unclear whether the mark plays a causal role in molecular or behavioral rhythmicity. To investigate this, we next performed Adeno-associated viral vector (AAV) transduction in TMN to introduce a mutant H3, H3.3Q5A, which is actively incorporated into neuronal chromatin **(Figure 4G)** and functions as a dominant negative, thereby reducing global levels of the mark (H3.3Q5A) (11). In these experiments, two AAV controls were transduced: an empty vector control expressing GFP and H3.3 WT, which were collapsed as a common control since H3.3 WT transduction did not alter H3Q5his expression *vs.* GFP **(Figure 4H, top)**. We additionally assessed H3K4me2 in response to viral transduction and found that its expression was anti-correlated with H3Q5his **(Figure 4H, bottom)**, consistent with the rhythmic expression data presented in **Figure 4D**. Finally, we examined what impact such perturbations may have on diurnal behavior, as assessed via locomotor activity across the ZT. Three weeks following viral transductions (the time required to achieve maximal expression of the viruses), mice were monitored for locomotor activity beginning 12 hours after a shift from light-dark (i.e., their normal housing conditions) to dark-dark in order to examine whether disrupting H3Q5his alters normal circadian cycling activities. Consistent with our hypothesis, we found that perturbing normal H3Q5his dynamics in TMN resulted in abnormal shifts in diurnal locomotor activity, particularly during transitions from inactive to active states, and vice versa **(Figure 4I)**. Subsequent RNA-seq on transduced TMN tissues confirmed significant overlaps with genes disrupted by H3Q5his manipulations in comparisons to those identified as being rhythmic in **Figure 1A-C**, as well as those predicted to be CLOCK gene targets

(Supplementary Figure 7D and Supplementary Data 2). In sum, our data revealed that not only is H3Q5his dynamic in its expression across the ZT but also that it contributes significantly to rhythmic gene expression and behavior.

H3Q5his antagonizes H3K4 methyltransferase activity through electrostatics

To investigate the potential biochemical mechanism governing H3Q5his' effect on H3K4 methylation dynamics during diurnal cycling – and, in turn, rhythmic gene expression and behavior – we next sought to explore whether H3Q5his may directly alter the activity of the H3K4 methylation machinery *in vitro*. Given that previous work, including our own, indicated that H3Q5ser can potentiate binding to WDR5 (8, 9, 25), an H3 "reader" protein and member of the MLL1 methyltransferase complex (26), we began by performing MALDI-TOF mass spectrometry on both unmodified H3 and H3Q5his peptides (1-15). We found that H3Q5his robustly attenuated MLL1 complex processivity to add methylation to H3K4 **(Figure 5A)**. These results were orthogonally confirmed using LC-MS/MS to monitor the establishment of H3K4 methylation states by MLL1 on H3 (1-21) unmodified *vs.* Q5ser *vs.* Q5his peptides, where we found that while H3Q5ser does not alter MLL1 activity *vs.* unmodified H3, H3Q5his significantly attenuates MLL1 complex activity (**Figure 5B-C**).

Based upon this attenuation, we next wished to explore the potential mechanisms responsible for this phenomenon. We began by modeling possible H3Q5his interactions with MLL using the published MLL3-RBBP5-ASH2L-H3 complex structure (27). Based upon our structural modeling assessments (**Figure 5D**), we predict that the H3Q5 residue would be 'sandwiched' between arginine (R) 4828 and K4887 of MLL3, and while enough space would exist, in theory, to tolerate a large modification, such as

serotonylation (with stacking between R4828 and serotonylation possibly stabilizing the H3 peptide; in addition, the double conformation of WDR5 F149 supports the notion that the binding surface of H3Q5ser is flexible, **Supplementary Figure 8**). However, the positively charged histaminylation moiety would not be favored owing to electrostatics. Additionally, since the MLL1 complex member WDR5 (which presents the H3 tail to MLL1 for deposition of H3K4 methylation) has previously been shown to interact with H3Q5 serotonylation through its WD repeats (9, 25), we next wished to assess whether H3Q5his may antagonize such interactions *vs.* H3Q5ser. We performed isothermal titration calorimetry (ITC) to measure interactions between the purified WD40 domain of WDR5 ($WDR5_{WD40}$) and the monoaminylated H3 tail (H3Q5ser *vs.* H3Q5his). As expected, $WDR5_{WD40}$ was found to bind to the unmodified H3 tail (K_D 20.20 μM), with a slight increase in binding observed in the context of a H3Q5ser substrate (K_D 14.01 μM). Interestingly, H3Q5his was observed to attenuate this binding (K_D 108.81 μM), reducing the affinity between H3 and $WDR5_{WD40}$ by ~5-fold **(Figure 5E**; see **Supplementary Table 1 for ITC statistics)**.

Since the MLL1 complex binds the H3 tail directly via interactions with WDR5, which can facilitate MLL1 methyltransferase activities (28), we next performed peptide IPs [H3 (1-10) unmodified *vs.* Q5his *vs.* Q5ser] against soluble nuclear extracts from HeLa cells. This was used to compare the interactions between the H3 peptides and members of the MLL1 complex (ASH2L, RBBP5 and WDR5) via western blotting. We found that while H3Q5ser significantly potentiates interactions between the MLL1 complex and the H3 tail, H3Q5his displayed abrogated binding (**Figure 5F** and quantified in **Figure 5H, left**). These results were orthogonally confirmed by performing peptide IPs against recombinant full length WDR5 (**Figure 5G** and quantified in **Figure 5H, right**).

Given that H3Q5his, unlike H3Q5ser, is positively charged at physiological pH, we next explored whether its charge may contribute to the inhibition of binding *vs.* H3Q5ser. To this end, we used X-ray crystallography to determine the structure of the $WDR5_{WD40}$-H3 complex in the presence of an H3Q5his peptide. While the electron density of H3Q5 was traceable within the structure, the density around the histamine moiety was not resolved **(Figure 5I,** and **Supplementary Table 2 for X-ray crystallography data collection and refinement statistics)**. We were, however, able to effectively model H3Q5his interactions based upon the orientation of the H3Q5 residue, restricted within the Ramachandran plot. This modeling indicated that while the H3R2 sidechain was inserted into the binding pocket of $WDR5_{WD40}$ (with the H3K4 sidechain at the surface of $WDR5_{WD40}$), as was shown previously (29), H3Q5his was predicted to display surface binding adjacent to the binding pocket. Additionally, the location of Q5 in proximity to the positively charged $WDR5_{WD40}$K259 residue in the structure suggested that $WDR5_{WD40}$K259 and H3Q5his may serve to electrostatically repel one another, thereby resulting in binding inhibition **(Figure 5J-K)**. To test this directly, we performed additional ITC analyses using $WDR5_{WD40}$ mutants. We found that while H3Q5his inhibits $WDR5_{WD40}$ binding to the H3 tail, $WDR5_{WD40}$K259A rescued this interaction **(Figure 5L;** see **Supplementary Table 1 for ITC statistics)**. Reciprocally, the $WDR5_{WD40}$K259E mutant displayed a slight increase in binding of $WDR5_{WD40}$ to H3Q5his.

In summary, we investigated the dynamics of monoamine installation by TGM2, which revealed that that these PTMs unexpectedly and directly compete. Mechanistically, this is due to the capacity of TGM2 to act as "writer," "eraser" and "re-writer" of the

monoaminylated moieties on H3. In fact, we found that TGM2 can utilize any of the monoamine cofactors examined on either unmodified or monoaminylated glutamines, a process that is primarily dependent on the microenvironmental concentrations of provided nucleophiles. Furthermore, when TGM2 "erases" the monoamine adduct in the absence of alternative donors, it leaves a glutamate at the site of modification, which results in a form of "protein-induced mutagenesis" that would likely prove deleterious to cellular function. As such, TGM2's "re-writing" activity on H3 likely represents a critical mechanism for maintaining cellular homeostasis during periods of intracellular monoamine fluctuations.

Leveraging this mechanistic insight, we identified a third class of H3 monoaminylation, histaminylation, which is also facilitated by TGM2 and occurs at the same site on H3 (Q5). Given previous evidence indicating that histamine levels in neonatal rodent brain are largely nuclear, the functions of which have remained elusive, we were interested in further exploring mechanistic roles for this new PTM *in vivo* (30). Using a new site-specific antibody that we developed, we found that H3Q5his expression is enriched at the site of histamine production in brain and showed that H3Q5his expression is dynamic in TMN as a function of sleep-wake cycles. These opposed patterns of H3K4 di-methylation, which have previously been implicated in circadian gene expression (23). Furthermore, we found that such dynamics can be disrupted by pharmacological manipulations of sleep behavior. In support, intra-TMN viral manipulations that reduce H3Q5his expression were found to disrupt normal patterns of locomotor activity during sleep-wake transitions, suggesting that the mark's dynamics may contribute to diurnal related phenotypes. Finally, based upon a series of biochemical and structural assessments, we found that H3Q5his, in comparison to H3Q5ser, attenuates MLL1

complex binding to the H3 tail. This is specifically governed by a predicted electrostatic repulsion (owing to H3Q5his' positive charge), and inhibits MLL1 complex mediated establishment of H3K4 methylation. Taken together, these data provide a previously unreported paradigm that addresses the dynamic regulation of histone monoaminylation events in cells/brain. Future studies aimed at elucidating TGM2's "re-writing" capabilities in brain (e.g., switching between H3 monoaminylation states within neural cell-type specific contexts to mediate chromatin state transitions that influence transcription) are warranted and may explain, at least in part, how monoamine dynamics – both adaptive and maladaptive – contribute to brain plasticity.

FIGURES AND LEGENDS

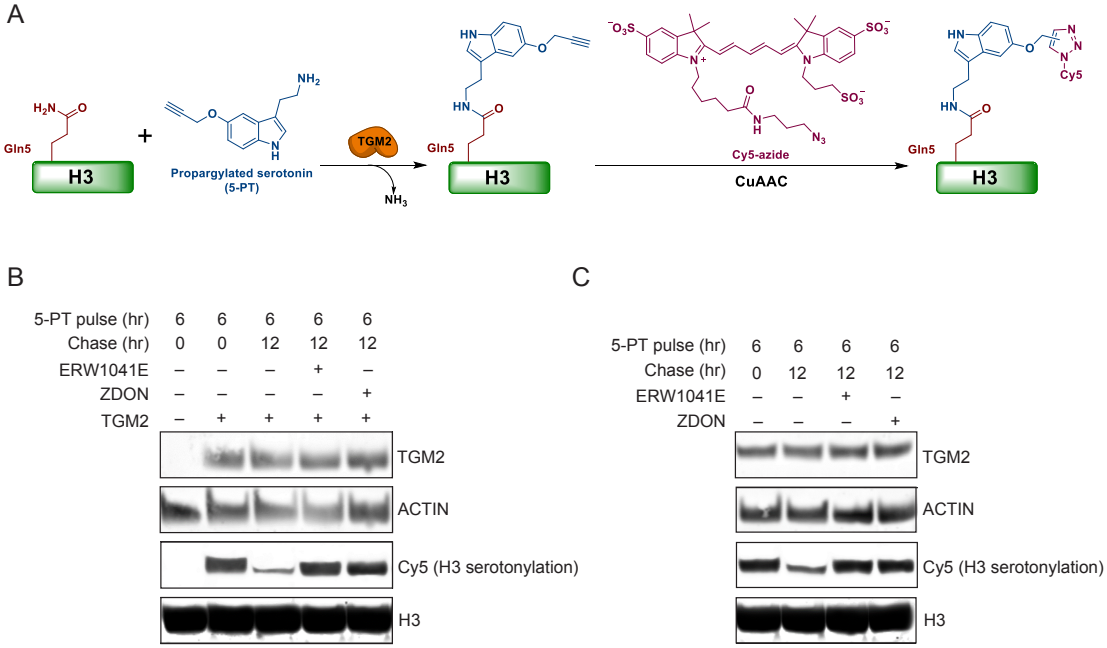

Figure 1. TGM2 is both necessary and sufficient for the addition and removal of H3 serotonylation *in cellulo*

(A) Schematic depicting TGM2 mediated covalent modification of H3Q5 by the serotonin analog, 5-PT, and its subsequent visualization via CuAAC-meditated Cyanine 5 (Cy5) conjugation. (B) 5-PT pulse/chase experiment in HEK293T cells, which do not endogenously express TGM2, transfected with TGM2-WT and treated -/+ TGM2 inhibitors (ERW1041E or ZDON) following the removal of 5-PT from the media. Western blotting was performed to examine Cy5 (i.e., H3 serotonylation) and TGM2 expression after media replacement -/+ TGM2 inhibition. Total H3 and ACTIN serve as loading controls. Experiment was repeated at least 3X. (C) 5-PT pulse/chase experiment in HeLa cells, which endogenously express TGM2, treated -/+ TGM2 inhibitors (ERW1041E or ZDON) following the removal of 5-PT from the media. Western blotting was performed to examine Cy5 (i.e., H3 serotonylation) and TGM2

expression after media replacement -/+ TGM2 inhibition. Total H3 and ACTIN serve as loading controls. Experiment was repeated at least 3X.

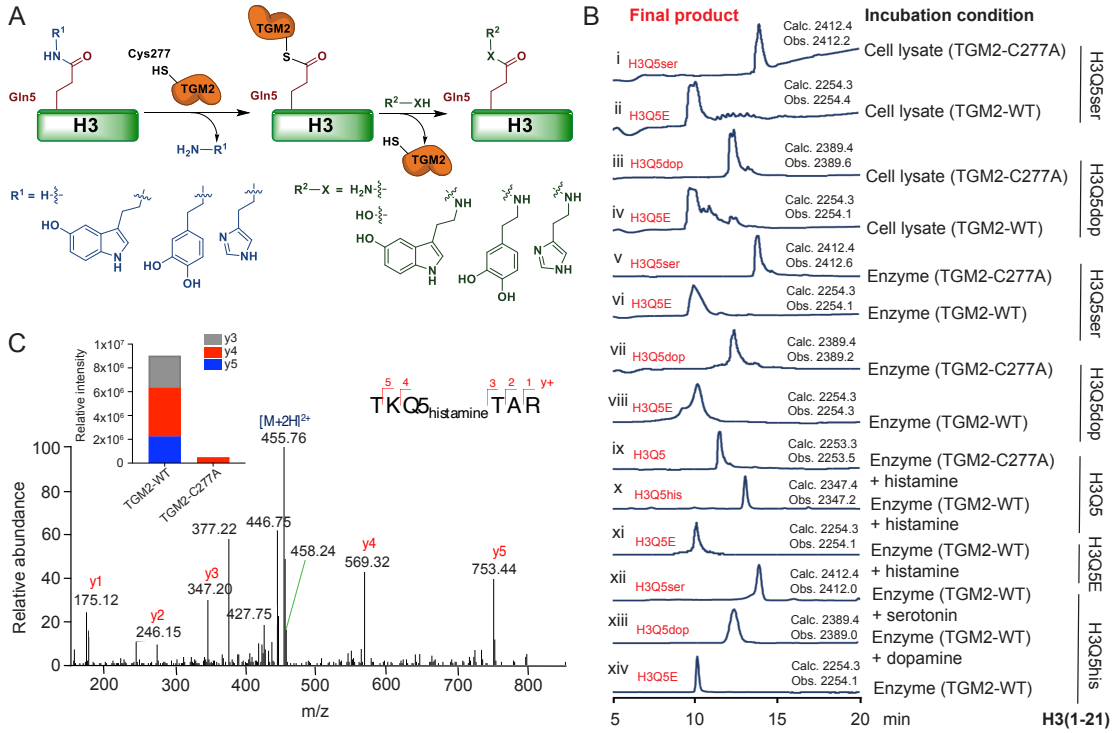

Figure 2. TGM2 "writes," "erases" and "re-writes" H3 monoaminylations *in vitro*

(A) Hypothesized mechanism of TGM2 mediated H3 monoaminylation 'writing,' 'erasing' and 're-writing.' In this model, TGM2's catalytic residue, cysteine (Cys) 277, attacks the γ-carboxamide group of glutamine 5 on H3, and the formation of a thioester intermediate structure then activates the amide bond to accept a nucleophilic attack from donors within the local microenvironment. (B) LC-MS analyses of synthetically modified H3 (1-21) peptides – H3Q5ser *vs.* H3Q5dop *vs.* H3Q5his (as well as an H3Q5E peptide standard for assessments of H3Q5 deamidation; xi) – following incubation with either cellular lysates expressing TGM2-WT or TGM2-C277A (i-iv) or recombinant TGM2-WT *vs.* TGM2-C277A (v-x). H3Q5his peptides were further incubated with TGM2-WT in the presence or absence of a replacement monoamine donor (xii – serotonin *vs.* xiii – dopamine), demonstrating that TGM2-WT can both deamidate H3 monoaminylations in the absence of a replacement donor (xiv) and 're-write' H3 monoaminylations in the presence of replacement donors. Calculated *vs.*

observed masses are provided. HPLC UV traces, λ = 214 nm. Experiment was repeated at least 3X. (C) LC-MS/MS analyses identified endogenous H3Q5his in HEK293T cells transfected with TGM2-WT following histamine treatments. y+ ions are annotated. Insert: Relative intensities of the most abundant *y* fragment ions from the H3Q5his peptide.

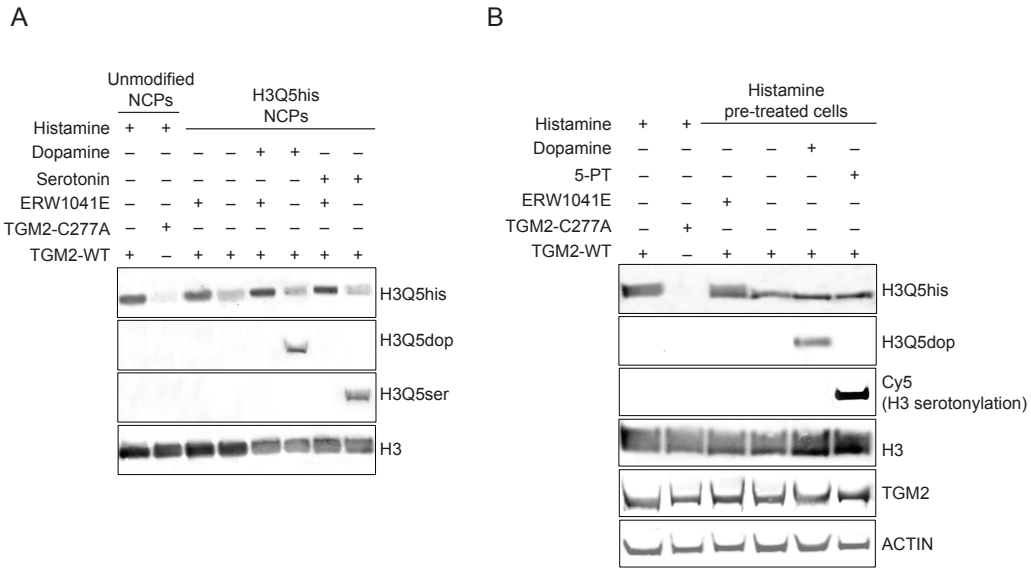

Figure 3. Noncanonical TGM2 mediated "re-writing" of H3 monoaminylations on NCPs and in cells

(A) TGM2-WT, but not TGM2-C277A, can transamidate histamine to H3Q5 on NCPs. NCPs pre-modified by histamine at H3Q5 can be deamidated by TGM2-WT, a mechanism that is inhibited by treatment with the TGM2 inhibitor ERW1041E. TGM2-WT can additionally 're-write' H3Q5his on NCPs in the presence of replacement monoamines donors, such as serotonin or dopamine, resulting in the establishment of H3Q5ser or H3Q5dop, respectively. Experiment repeated at least 3X. (B) TGM2-WT, but not TGM2-C277A, can transamidate histamine to H3Q5 in HEK293T cells. H3Q5his pre-modified histones can be deamidated by TGM2-WT *in cellulo*, a mechanism that is inhibited by treatment with the TGM2 inhibitor ERW1041E. TGM2-WT can also 're-write' H3Q5his *in cellulo* in the presence of replacement monoamines donors, such as 5-PT (serotonin analog; assessed via Cy5 conjugation) or dopamine, resulting in the establishment of H3 serotonylation or H3Q5dop, respectively. Total H3

and ACTIN western blots are provided as loading controls. Experiment repeated at least 3X.

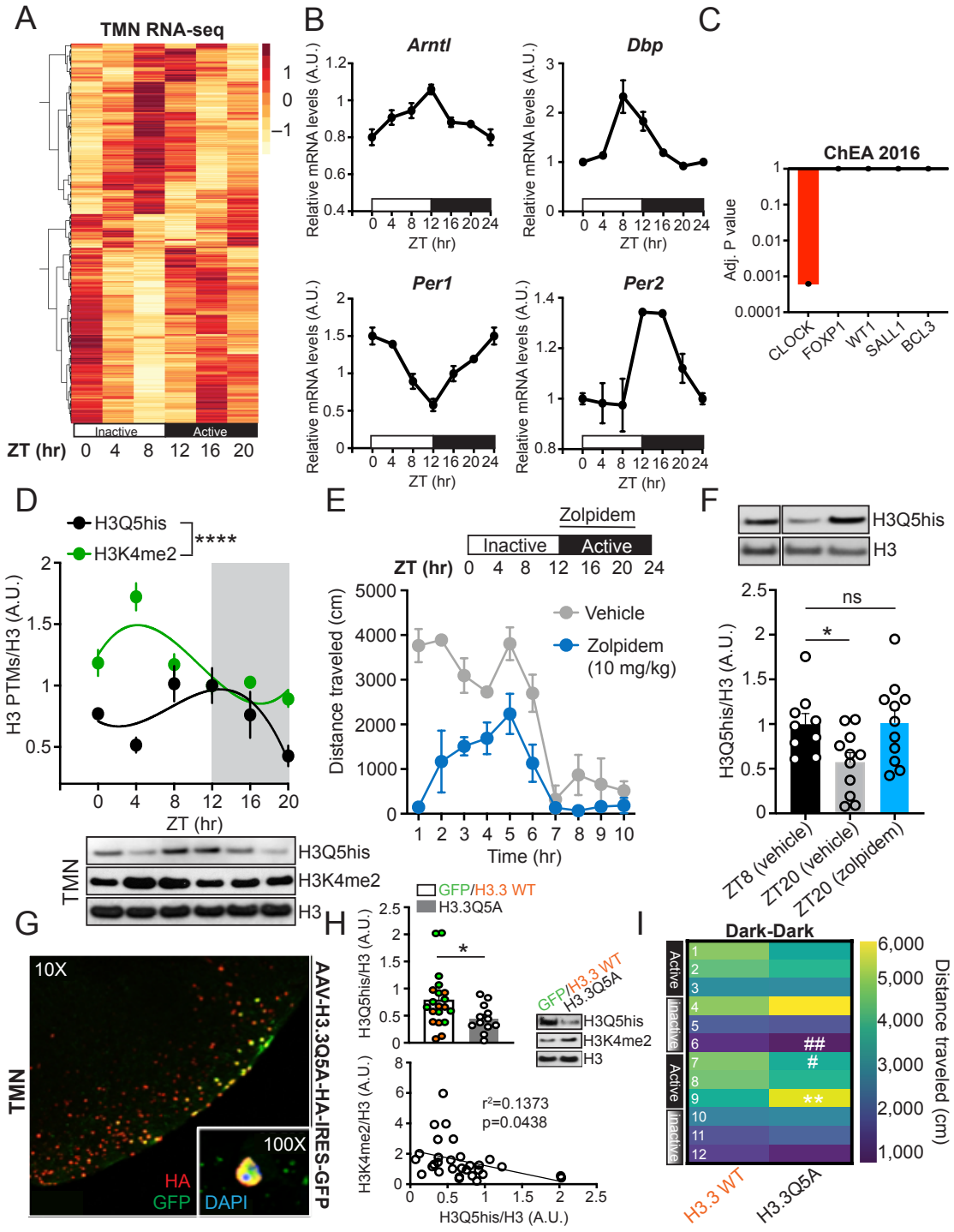

Figure 4. Diurnal H3Q5his dynamics in TMN contribute to neural rhythmicity

(A) RNA-seq of mouse TMN across the ZT (tissues collected at ZT 0, 4, 8, 12, 16 and 20) identifies rhythmic patterns of gene expression (*n*=3 biological replicates/time point), (B) including known circadian genes, such as *Arntl*, *Dbp*, *Per1* and *Per2*. (C) ChEA analysis reveals the transcription factor CLOCK as an important contributor to

rhythmic genes identified in TMN. (D) H3Q5his in TMN displays a rhythmic pattern of expression across the ZT in mice [*n*=8-10 per time point; comparison of fits analysis between third order polynomial, cubic trend (alternative hypothesis), *vs.* first order polynomial, straight line (null hypothesis) – p=0.0034, null hypothesis rejected], a pattern that significantly diverges from that of adjacent H3K4me2 (p<0.0001), a mark that also displays rhythmic expression in this brain region (*n*=6-10 per time point; comparison of fits between third order polynomial, cubic trend (alternative hypothesis), *vs.* first order polynomial, straight line (null hypothesis) – p=0.0079, null hypothesis rejected]. H3 western blots are provided as loading control. (E) Assessments of locomotor activity in mice treated with Zolpidem *vs.* vehicle during their active phase (*n*=10/group). (F) Examination of H3Q5his in TMN of mice treated with Zolpidem *vs.* vehicle during their active phase at ZT8 (vehicle, *n*=9) and ZT 20 (Zolpidem *vs.* vehicle, (*n*=11/group) – one-way ANOVA (p=0.0227, Dunnett's post hoc test, *p<0.05. H3 western blots are provided as loading control. (G) IHC/IF analysis confirming nuclear expression of H3.3Q5A-HA dominant negative in TMN of mice expressing AAV-H3.3Q5A-HA-IRES-GFP. (H) Top – Western blot validation of H3Q5his downregulation in TMN following AAV mediated expression of H3.3Q5A *vs.* H3.3WT or empty vector controls (*n*=9-12/viral treatment group – control groups collapsed; unpaired student's t-test, *p=0.0422). Bottom – Linear regression analysis comparing intra-animal H3Q5his *vs.* H3K4me2 expression in TMN following viral infections with vectors expression H3.3Q5A *vs.* H3.3 WT or empty vector controls (*n*=9-12/viral treatment group). H3 western blots are provided as loading control for both marks. (I) Following intra-TMN transduction with H3.3Q5A *vs.* H3.3 WT, mice were monitored for locomotor activity beginning 12 hours after a shift from light-dark to dark-dark to examine whether disrupting H3Q5his alters normal circadian cycling activities.

Disrupting normal H3Q5his dynamics in TMN resulted in abnormal shifts in diurnal locomotor activity during transitions from inactive to active states, and vice versa. Heatmap presents locomotor data binned into 4-hour intervals for a total of 48 hours [*n*=10-11/viral group, two-way ANOVA, interaction of time x virus – **p=0.0040, Sidak's multiple comparison test – **p=0.0079, *a posteriori* Student's t-test – #p<0.05, ##p<0.01]. Data are represented as mean ± SEM.

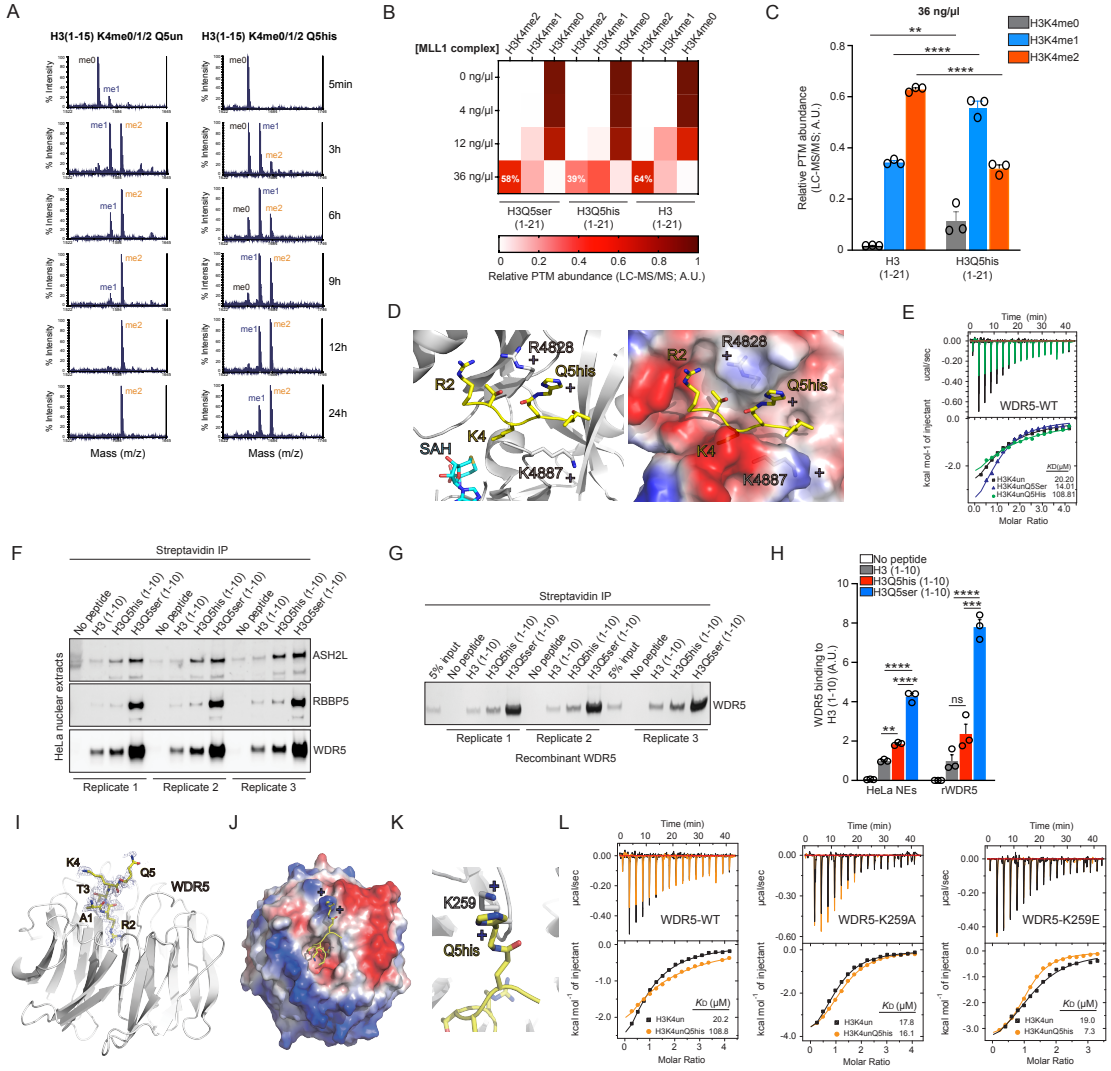

Figure 5. H3Q5his antagonizes MLL1 mediated H3K4 methylation establishment via electrostatics

(A) MALDI-TOF assessments of the recombinant MLL1 complex methyltransferase activities on H3K4 comparing H3K4unmodQ5unmod *vs.* H3K4unmodQ5his peptides (1-15). (B) LC-MS/MS quantification of H3K4 methylation states (H3K4me0 *vs.* H3K4me1 *vs.* H3K4me2; H3K4me3 signal was negligible and was thus omitted) on H3 (1-21) unmodified *vs.* H3Q5ser *vs.* H3Q5his peptides, titrating the concentration of MLL1 complex in the system. (C) LC-MS/MS quantification of H3K4 methylation states (H3K4me0 *vs.* H3K4me1 *vs.* H3K4me2; H3K4me3 signal was negligible and was thus omitted) on H3 (1-21) unmodified *vs.* H3Q5ser *vs.* H3Q5his peptides using

36 ng/ul of MLL1 complex with replicates (n = 3) for quantification. Two-way ANOVA with Sidak's multiple comparison test; **p<0.01, ****p<0.0001. (D) The catalytic center of MLL3 (PDB ID: 5F6K). The H3Q5his modification was modeled into the structure. (E) ITC assessments of $WDR5_{WD40}$ binding to H3K4unmodQ5unmod *vs.* H3K4unmodQ5his *vs.* H3K4unmodQ5ser peptides. (E) ITC assessments of $WDR5_{WD40}$ binding to H3K4unmodQ5unmod *vs.* H3K4unmodQ5his *vs.* H3K4unmodQ5ser peptides. (F) Peptide IPs [H3 (1-10) unmodified *vs.* Q5his *vs.* Q5ser] against soluble nuclear extracts from HeLa cells comparing their interactions with members of the MLL1 complex (ASH2L, RBBP5 and WDR5) via western blotting. (G) Results from (F) were orthogonally confirmed by peptide IPs against recombinant full length WDR5. (H) Quantification of binding data from (F-G). Within experiment one-way ANOVAs followed by Tukey's multiple comparison tests; **p<0.01, ***p<0.001, ****p<0.0001. (I) X-ray crystal structure of the $WDR5_{WD40}$-H3 complex demonstrated that H3Q5 displays flexible surface binding with $WDR5_{WD40}$. (J-K) The location of Q5 near the positively charged $WDR5_{WD40}$K259 residue in the structure indicated that $WDR5_{WD40}$K259 and H3Q5his may serve to electrostatically repel one another, resulting in binding inhibition. (L) Left – ITC assessments of $WDR5_{WD40}$ binding to H3K4unmodQ5unmod *vs.* H3K4unmodQ5his peptides. Middle – ITC assessments of $WDR5_{WD40}$K259A binding to H3K4unmodQ5unmod *vs.* H3K4unmodQ5his peptides. Right – ITC assessments of $WDR5_{WD40}$K259E binding to H3K4unmodQ5unmod *vs.* H3K4unmodQ5his peptides.

ACKNOWLEDGEMENTS

We would like to thank members of the Maze and David laboratories for critical readings of the manuscript. This work was partially supported by grants from the National Institutes of Health: R01 MH116900 (I.M.), R35 GM138386 (Y.D.), P30 CA008748 (Y.D.), P50 CA192937 (Y.D.), T32 DA007135 (R.M.B.), S10 OD030286 (S.S.), P30 CA013330 (S.S.), R37 GM086868 (T.W.M.), as well as funds from OSUCCC (Q.Z.), AFAR (Sagol Network GerOmics award; S.S.), Deerfield (Xseed award; S.S.), Relay Therapeutics (S.S.), Merck (S.S.), and the Einstein-Mount Sinai Diabetes Research Center (S.S.). The David Lab is also supported by the Josie Robertson Foundation, the Pershing Square Sohn Cancer Research Alliance, the Parker Institute for Cancer Immunotherapy, the STARR Cancer Alliance award, and the Anna Fuller Trust. In addition, the David lab is supported by W. H. Goodwin, A. Goodwin, and the Commonwealth Foundation for Cancer Research and the Center for Experimental Therapeutics at MSKCC.

Contributions

I.M., Y.D. and H.L. conceived of the project with input from Q.Z., R.M.B, S.Z., & T.W.M. Q.Z., R.M.B., S.Z., S.S., H.L., Y.D., & I.M. designed the experiments and interpreted the data. Q.Z., R.M.B., S.Z., L.K., L.V., H.F., B.Z., R.E.T., H.M., S.S., S.S., T.W.M., H.L., Y.D. & I.M. collected and analyzed the data. A.R. & L.S. performed the sequencing-based bioinformatics with input from S.L.F. Q.Z., R.M.B., H.L., Y.D. & I.M. wrote the manuscript with input from other authors.

Data availability

The RNA-seq data generated in this study have been deposited in the National Center for Biotechnology Information Gene Expression Omnibus (GEO) database under

accession number GSE209834. Raw files for the H3Q5his mass spectrometry proteomics data in 293T cells have been deposited to the Chorus repository under project #1782. The atomic coordinates and structure factors have been deposited in the Protein Data Bank (PDB) under PDB ID code 8HMX. We declare that the data supporting findings for this study are available within the article and Supplementary Information. Related data are available from the corresponding author upon reasonable request. No restrictions on data availability apply.

Competing interests

The Authors declare no competing interests

REFERENCES AND NOTES

1. G. Millán-Zambrano, A. Burton, A. J. Bannister, R. Schneider, *Nat. Rev. Genet.* **23**, 563-580 (2022).
2. B. D. Strahl, C. D. Allis, *Nature* **403**, 41-45 (2000).
3. T. Jenuwein, C. D. Allis, *Science* **293**, 1074-1080 (2001).
4. J. Fan, K. A. Krautkramer, J. L. Feldman, J. M. Denu, *ACS Chem. Biol.* **10**, 95-108 (2015).
5. Q. Zheng, N. A. Prescott, I. Maksimovic, Y. David, *Chem. Res. Toxicol.* **32**, 796-807 (2019).
6. Q. Zheng, I. Maksimovic, A. Upad, Y. David, *Protein Cell* **11**, 401-416 (2020).
7. J. C. Chan, I. Maze, *Trends Biochem. Sci.* **45**, 829-844 (2020).
8. L. A. Farrelly *et al.*, *Nature* **567**, 535-539 (2019).
9. S. Zhao *et al.*, *Proc. Natl. Acad. Sci. U. S. A.* **118**, e2016742118 (2021).
10. A. E. Lepack *et al.*, *Science* **368**, 197-201 (2020).
11. S. L. Fulton *et al.*, *Neuropsychopharmacology* **368**, DOI: 10.1038/s41386-022-01279-4 (2020).
12. B. J. Lukasak *et al.*, *Proc. Natl. Acad. Sci. U. S. A.* **119**, e2208672119 (2022).
13. L. Lorand, R. M. Graham, *Nat. Rev. Mol. Cell Biol.* **4**, 140-156 (2003).

14. L. Fesus, M. Piacentini, *Trends Biochem. Sci.* **27**, 534-539 (2002).

15. J. C.-Y. Lin *et al.*, *Chembiochem* **14**, 813-817 (2013).

16. L. Dafik, C. Khosla, *Chem. Biol.* **18**, 58-66 (2011).

17. S. J. McConoughey *et al.*, *EMBO Mol. Med.* **2**, 349-370 (2010).

18. E. Tiligada, M. Ennis, *Br. J. Pharmacol.* **177**, 469-489 (2020).

19. T.-S. Lai, C. S. Greenberg, *Amino Acids* **45**, 857-864 (2013).

20. A. Fujita *et al.*, *J. Neurosci.* **37**, 9574-9592 (2017).

21. M. E. Hughes, J. B. Hogenesch, K. Kornacker, *J. Biol. Rhythms.* **25**, 372-380 (2010).

22. A. Lachmann *et al.*, *Bioinformatics* **26**, 2438-44 (2010).

23. H. Raduwan, A. L. Isola, W. J. Belden, *J. Biol. Chem.* **288**, 8380-8390 (2013).

24. M. H. Hastings, E. S. Maywood, M. Brancaccio, *Nat. Rev. Neurosci.* **19**, 453-469 (2018).

25. J. Zhao *et al.*, *Sci. Adv.* **7**, eabf4291 (2021).

26. R. C. Trievel, A. Shilatifard, *Nat. Struct. Mol. Biol.* **16**, 678-680 (2009).

27. Y. Li *et al.*, *Nature* **530,** 447-452 (2016).

28. Z. Odho, S. M. Southall, J. R. Wilson, *J. Biol. Chem.* **285**, 32967-32976 (2010).

29. J.-J. Song, R. E. Kingston, *J. Biol. Chem.* **283**, 35258-35264 (2008).

30. A. B. Young, C. D. Pert, D. G. Brown, K. M. Taylor, S. H. Snyder, *Science* **173**, 247-249 (1971).